ELSEVIER

Sensors and Actuators A 101 (2002) 231–238

SENSORS AND ACTUATORS A PHYSICAL

www.elsevier.com/locate/sna

Robust capacitive pressure sensor array

Sung-Pil Chang*, Jeong-Bong Lee[1], Mark G. Allen

School of Electrical and Computer Engineering, Georgia Institute of Technology, Atlanta, GA 30332-0250, USA

Received 10 August 2001; accepted 29 May 2002

Abstract

Much of the cost of commercial micromachined pressure sensors lies in the package that houses the device itself. If a robust material is used for the substrate of the sensors as well as the packaging material, i.e. fabricating the sensor on the package itself, cost savings for the overall system may accrue. In this work, stainless steel has been studied as a potential robust substrate for micromachined devices. Lamination process techniques combined with traditional micromachining processes have been investigated as suitable fabrication technologies. To illustrate these principles, capacitive pressure sensor arrays have been designed, fabricated, and characterized. Each array uses a stainless steel substrate, a laminated film as a suspended movable plate, and a fixed, surface micromachined back electrode of electroplated nickel. Three candidate diaphragm materials: Kapton polyimide film; stainless steel; and titanium, have been considered. Sensitivities of devices fabricated using these technologies range from 9.03–294.75 ppm/kPa. An important attribute of this design is that only the steel substrate and the pressure sensor inlet is exposed to the environment; i.e. the sensor is self packaged.
© 2002 Elsevier Science B.V. All rights reserved.

Keywords: Capacitive pressure sensor; Robust substrate; Lamination; Micromachining

1. Introduction

Since the root of micromachining technology is in integrated circuit processing, micromachined devices have been primarily realized using silicon substrates [1–4]. In many applications, these silicon-based devices are then protected mechanically against harsh environments by use of a robust packaging material [5,6]. However, this approach often leads to systems in which the cost of the package equals or exceeds the cost of the micromachined device itself. If this robust packaging material is directly used not only as the packaging or housing, but also as the substrate of the micromachined devices, many of the steps of the packaging process might be reduced, potentially leading to cost savings. Another potential advantage is that due to substrate robustness, these co-packaged devices may be able to be used in mechanically harsh environments, such as aerospace and oceanography applications.

In this work, we have investigated the use of robust substrates as suitable starting points for both bulk and surface micromachined structures, as well as investigated the possibility of the substrate forming essential structural components of the device package. Alternative fabrication techniques, such as those commonly used in conventional machining and electronic packaging fabrication, are combined with traditional integrated circuit-based microelectronics processing techniques to create micromachined devices on these robust substrates. To illustrate these principles, robust capacitive pressure sensors were fabricated using stainless steel as the substrate, laminated materials as the pressure sensitive diaphragm, and electroplated nickel as the back electrode. An important attribute of this design is that only the stainless steel substrate and the pressure sensor inlet are exposed to the environment, i.e. the sensor is self packaged. Three candidate diaphragm materials: Kapton polyimide film; stainless steel; and titanium, have been considered. Polymer diaphragms offer the potential for high sensitivity at low pressure [7]. However, one potential issue with polymer diaphragms is the absorption of moisture from the environment into the film. In order to circumvent this issue, metal diaphragms of stainless steel and titanium are also investigated.

The principle of operation is based on the pressure-induced deflection of a diaphragm and the subsequent measurement of the capacitance between this deflecting diaphragm and a fixed backplate surface micromachined over the deflecting diaphragm. Fig. 1 shows a schematic cross-section of the device, where t_g is the initial (undeflected) gap distance between the fixed back electrode and the diaphragm

* Corresponding author.
E-mail address: gt6586a@prism.gatech.edu (S.-P. Chang).
[1] Present address: Erik Jonsson School of Engineering and Computer Science, University of Texas, Dallas, Richardson, TX 75083-0688, USA

0924-4247/02/$ – see front matter © 2002 Elsevier Science B.V. All rights reserved.
PII: S0924-4247(02)00193-0

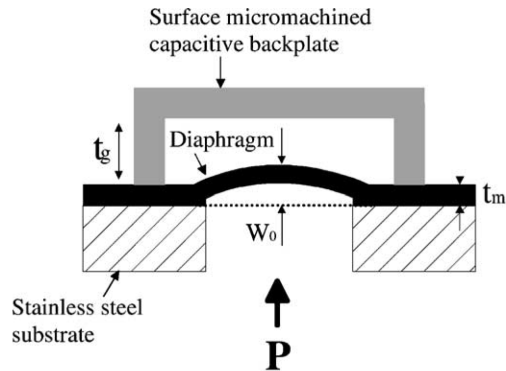

Fig. 1. A schematic diagram of the side view of the capacitive pressure sensor.

electrode, w_0 is the deflection at the center of the diaphragm, t_m is the thickness of the diaphragm, and P is the uniform applied pressure.

2. Fabrication process

2.1. Fabrication of kapton diaphragm pressure sensors

The fabrication sequence of the capacitive pressure sensor array is shown in Fig. 2. The process starts on square 5.7 cm (214 in.) on a side, 0.5 mm thick stainless steel substrate that has surface roughness of approximately 6–8 μm. An array of 8×8 pressure inlet holes with a diameter of 2 mm, with 5 mm center-to-center distances, is milled through the stainless steel substrate. Kapton polyimide film (Dupont, Kapton HN200, 50 μm thick) is laminated onto the milled stainless steel substrate using a hot press with a pressure of 8.65 MPa and a temperature of 175 °C for 30 min. The laminate adhesive is an epoxy-based resin designed for printed wiring board fabrication (EIS epoxy laminate prepreg #106). The pressure-sensitive diaphragms will be the Kapton polyimide film in the regions suspended over the milled pressure inlet holes (Fig. 2a).

A triple metallic layer of Ti/Cu/Ti with a thickness of 100/2000/500 Å is deposited by electron-beam evaporation and then patterned using a lift-off process to create bottom electrodes, electroplating seed layers, and bonding pads on the surface of the Kapton polyimide film (Fig. 3a). Multiple layers of PI2611 polyimide (Dupont) are spun onto the patterned layer with a spin speed of 1200 rpm for 60 s, and hard-cured in a N_2 ambient at 200 °C for 120 min yielding a final thickness of polyimide of approximately 44–48 μm.

The polyimide layer is anisotropically etched using reactive ion etching (RIE) to create electroplating molds for the support posts of the fixed backplates, and to remove the uppermost titanium layer of the seed layer (Fig. 2b). Nickel supports are then electroplated through the polyimide molds.

A Ti/Cu/Ti metallic triple layer with a thickness of 300/2000/300 Å is deposited using dc sputtering to act as a seed layer for the deposition of the backplate. Thick photoresist (Shipley SJR 5740) is spun on the seed layer with a spin speed of 1100 rpm for 30 s (yielding a final thickness of approximately 15 μm) and patterned to act as electroplating molds for the backplates. After removal of the uppermost Ti layer, nickel is electroplated through the thick photoresist electroplating molds to create the backplates (Fig. 2c). The thick photoresist electroplating molds and the remaining seed layer is removed. Finally, the polyimide molds for the backplate posts as well as polyimide sacrificial layers are isotropically etched to create air gaps between the fixed backplates and the pressure sensitive Kapton polyimide flexible diaphragms (Figs. 2d and 3c). The isotropic dry etch is carried out in a barrel plasma etcher using CF_4/O_2 plasma with a RF power of 120 W. Fig. 3 shows photographs of a fabricated pressure sensor array, where (b) shows a side view and (c) shows a close-up view of the gap defined between the fixed backplate and the diaphragm. Note that these sensors are operating in differential mode, with the side containing the backplate held at a pressure of 1 atm.

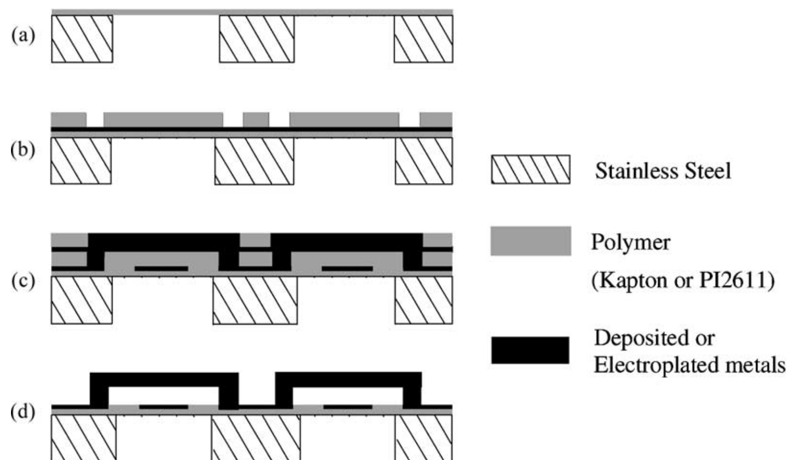

Fig. 2. Fabrication sequence of pressure sensor based on Kapton polyimide diaphragm.

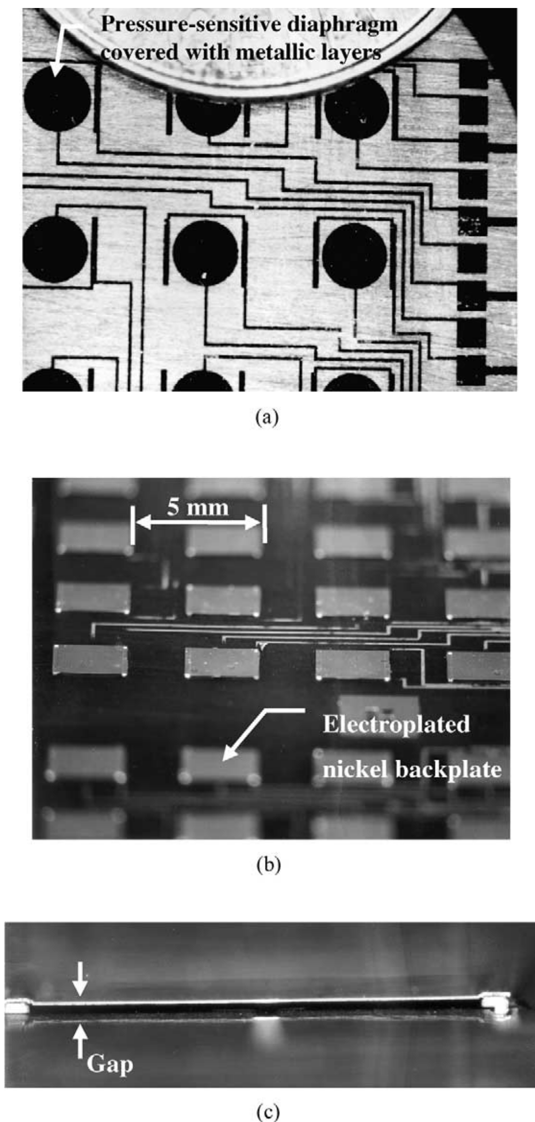

Fig. 3. Photographs of fabricated pressure sensor array: (a) a photograph of top-view of the metallic seed layer; (b) a side view of the pressure sensor array; (c) a close-up view of the gap (approximately 44 μm) defined between electroplated nickel backplate and pressure sensitive Kapton polyimide diaphragm.

2.2. Fabrication of stainless steel diaphragm pressure sensors

The fabrication sequence of stainless steel diaphragm pressure sensors is shown in Fig. 4. The process starts on square, stainless steel substrates that are each 6.0 cm on a side, 0.8 mm thick, and have surface roughness of approximately 6–8 μm. A 6 × 6 array of pressure inlet holes with a diameter of 2 mm, with 7 mm center-to-center distances, is milled through the stainless steel substrates. A stainless steel sheet (Precision Brand Product, Inc.) is laminated onto the milled stainless steel substrate using a hot press with a pressure of 8.65 MPa and a temperature of 175 °C for 30 min. The stainless steel sheet is used as the pressure sensitive diaphragm and has a thickness of 12.7 μm and surface roughness of approximately 100 Å. RIE is then used to remove any exposed epoxy resin under the stainless steel diaphragm that has leaked through the pressure inlet holes (Fig. 4a).

A 250 Å thick titanium layer is deposited as an adhesion layer, and a 7 μm thick epoxy resist SU 8-2 (MicroChem Corp.) is deposited as an insulation layer. To create bottom electrodes, electroplating seed layers, and bonding pads, Ti/Cu/Ti layers are deposited with a thickness of 250/6000/250 Å and patterned. AZ 4620 photoresist (Clariant Corp.) is spun onto the patterned layer, yielding a final thickness of photoresist of approximately 25–27 μm (Fig. 4b). The photoresist is patterned to create electroplating molds and nickel supports are electroplated through the molds.

To fabricate the backplate, a seed layer of Ti/Cu/Ti is deposited. Thick photoresist (AZ 4620) is spun on the seed layer (approximately 25 μm thick) and patterned to form electroplating molds. These molds are then filled with nickel by electroplating (Fig. 4c). Finally, the photoresist sacrificial layers and the seed layers between them are etched to release the gap between the fixed backplate and the pressure sensitive stainless steel diaphragm (Fig. 4d). Fig. 5 shows a photomicrograph of the fabricated stainless steel sensor array.

2.3. Fabrication of titanium diaphragm pressure sensors

The fabrication sequence of the titanium diaphragm pressure sensors is similar to that of the stainless steel diaphragm pressure sensor devices. The same stainless steel substrates and epoxy lamination adhesives as those used in the stainless steel diaphragm devices fabrication process are used. Instead of a stainless steel sheet, a titanium film (Teledyne Rodney Metals, type Ti 540) which has 25.4 μm thickness and surface roughness of approximately 60 Å is then laminated on the stainless steel substrates using a hot press under the same conditions as that of the stainless steel diaphragm sensor process. The fabrication sequence after lamination of this titanium film is the same as that of the stainless steel diaphragm sensors except for the lack of a titanium deposition step for SU 8-2 adhesion promotion since the substrate material itself is titanium.

3. Theoretical model

For mechanical modeling, several assumptions have been made: (a) the diaphragm has isotropic mechanical properties; (b) the thickness of the metallic electrode on the plate has been neglected, since this thickness is small compared with the plate thickness; (c) electric field fringing effects have been neglected, since the gap between the flexible diaphragm and the fixed backplate is small compared to their lateral extents; (d) residual stress in the diaphragm can be neglected. Under these conditions, the deflection of a circular diaphragm with

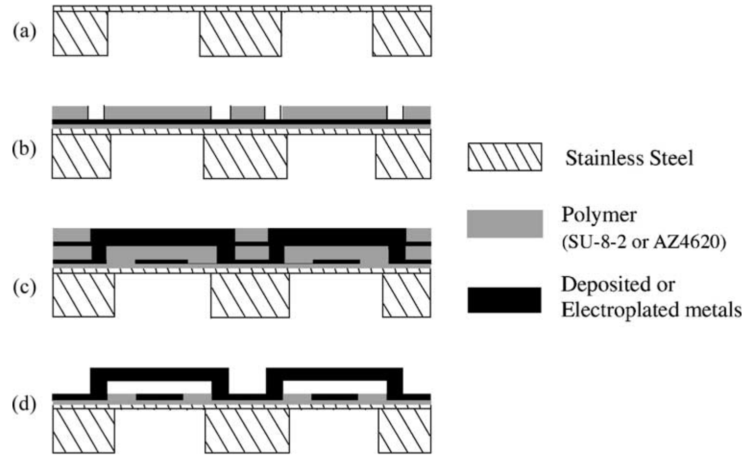

Fig. 4. Fabrication sequence of pressure sensor based on stainless steel diaphragm.

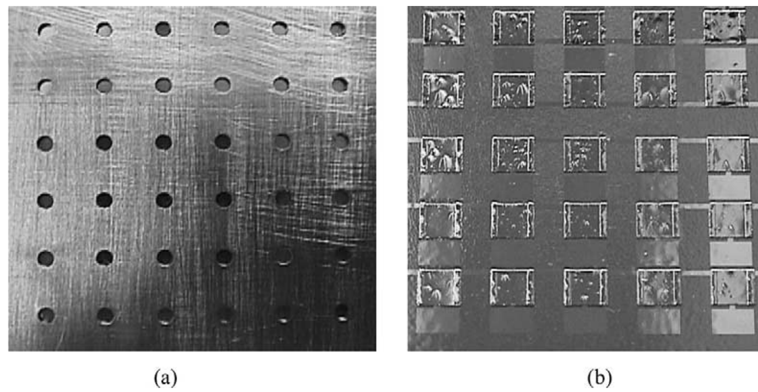

Fig. 5. Photomicrographs of fabricated pressure sensors: (a) side exposed to environment; (b) rear view showing surface micromachined backplate.

fully clamped perimeter as a function of radius, $w(r)$, is given by [8,9]:

$$w(r) = w_0\left[1-\left(\frac{r}{a}\right)^2\right]^2 \tag{1}$$

where a is the radius of the plate. The center deflection of the plate w_0 is given by the solution to the Eq. (2) [10].

$$\frac{Pa^4}{Et_{\rm m}^4} = \frac{16}{3(1-\mu^2)}\frac{w_0}{t_{\rm m}} + \frac{7-\mu}{3(1-\mu)}\frac{w_0^3}{t_{\rm m}^3} \tag{2}$$

where E is the modulus of elasticity and μ is the Poisson ratio of the plate and $t_{\rm m}$ is the thickness of diaphragm.

If the deflections are small compared with the thickness, the Eq. (2) reduce to [8]:

$$w_0 = \frac{3Pa^4(1-\mu^2)}{16Et_{\rm m}^3} \tag{3}$$

As the electric field fringing effect is neglected under the assumption (c), the electric field lines are perpendicular to the surface of the back plate and the capacitance can be expressed as a function of the shape function $w(r)$ of the membrane by

$$C_{\rm s} = \varepsilon_0\int_0^{2\pi}{\rm d}\theta\int_0^r {\rm d}r\frac{r}{t_{\rm g}-w(r)} \tag{4}$$

we replace $w(r)$ in Eq. (4) using Eq. (1) and replace w_0 by the dimensionless parameter

$$\gamma = \frac{w_0}{t_{\rm g}} \tag{5}$$

then we replace the integration variable r by the dimensionless variable

$$x = \sqrt{\gamma}\left[1-\left(\frac{r}{a}\right)^2\right] \tag{6}$$

This yields

$$C = \varepsilon_0\frac{\pi a^2}{t_{\rm g}}\gamma^{-0.5}\int_0^{\sqrt{\gamma}}\frac{{\rm d}x}{1-x^2} \tag{7}$$

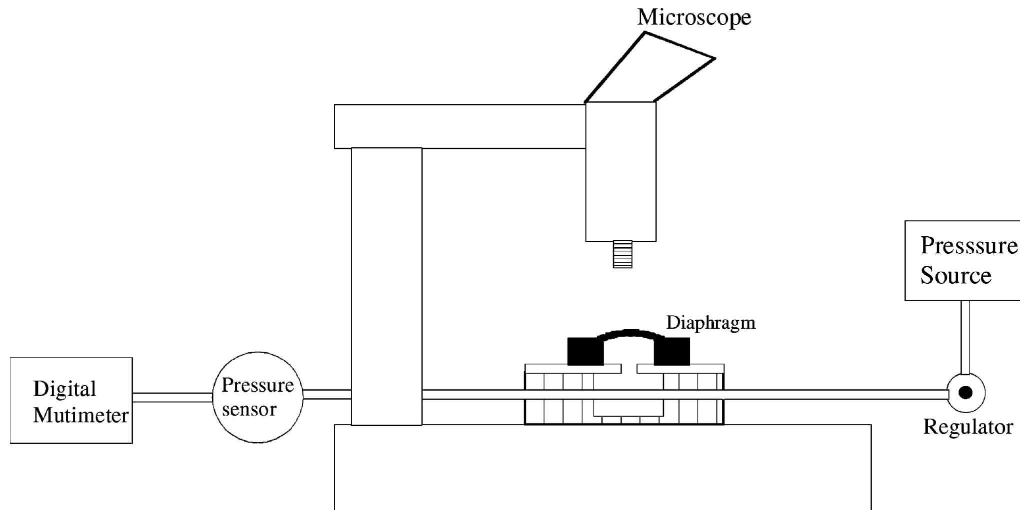

Fig. 6. Optical diaphragm deflection measurement setup.

Finally, we solve the integral and use the capacitance when the membrane is undeflected

$$C_0 = \varepsilon_0 \frac{\pi a^2}{t_g} \tag{8}$$

which yields

$$C = C_0 \gamma^{-0.5} \tanh^{-1}(\gamma^{0.5}) \approx C_0 \left(1 + \frac{\gamma}{3} + \frac{\gamma^2}{5}\right) \tag{9}$$

where the second part of Eq. (9) was obtained from the fifth-order Taylor series expansion of $\tanh^{-1}(y)$.

Eqs. (2) and (3) relates the pressure of the diaphragm to deflection, while Eq. (9) relates the deflection of the diaphragm to the capacitance of the sensor. If the diaphragms follow Eqs. (2) and (3), the mechanical behavior can be combined into Eq. (9) using Eq. (5). If they do not, a direct measurement of deflection versus pressure can be used in conjunction with Eqs. (5) and (9) to predict the capacitance versus pressure behavior of the sensors.

4. Characterization results

In order to characterize the capacitance of individual pressure sensors, measurements were carried out with a Keithley 3322 LCZ meter. The sensor device to be tested was mounted and sealed on a test fixture. The fixture was connected to a commercial pressure sensor (Fluke Corp. PV 350 Digital Pressure/Vacuum Module) and a digital multimeter to monitor the differential pressure. A compressed nitrogen line was connected to the fixture to serve as the pressure source with a regulator between them to control the differential pressure that would be applied to the fabricated devices. The LCZ meter was then connected to the fabricated sensors to obtain the characterization data for the capacitive pressure sensor.

After collection of the capacitance data, to measure the membrane deflections directly, the electroplated NiFe over the membrane was removed and the exposed membrane was then placed on a microscope stage. Pressure was then applied to the membranes through the fixtures and the resultant deflection of the membrane was observed and measured with the microscope, by measuring with a z-axis micrometer. It is necessary to constantly adjust the microscope head to keep the deflected diaphragm in focus. The test setup is shown in Fig. 6. By adjusting the input pressure and the focus position, the center deflection of the diaphragm could be measured to a resolution of ±0.4 μm.

4.1. Kapton diaphragm sensors

The data obtained with Kapton diaphragm sensors are shown in Fig. 7. Measured capacitances for undeflected pressure sensors were in the range of 11.35–13.97 pF depending on the length of interconnections between bonding pads and sensors. Over an applied pressure range from 0

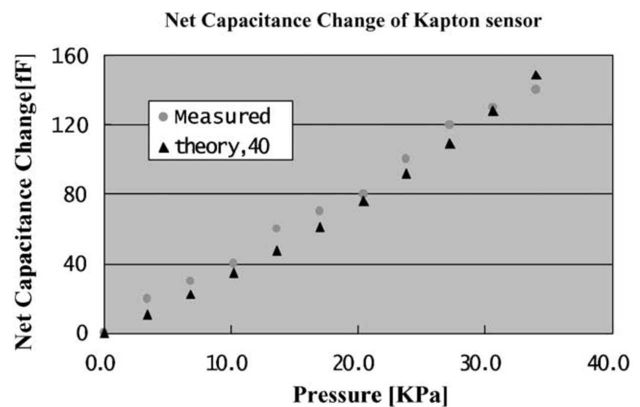

Fig. 7. Net capacitance change vs. pressure for Kapton diaphragm pressure sensor.

to 34 kPa, the net capacitance change was approximately 0.14 pF. This corresponds to an average absolute sensitivity of 294.75 ppm/kPa. Theoretical prediction of the sensor behavior is determined by taking the first three terms of Eq. (9) using Eqs. (3) and (5) to calculate γ. The theoretical data shown in Fig. 7 is based on an initial gap (d_1) of 40 μm. There is approximately a 10–20% difference between the measured physical gap and the 40 μm gap value used to provide a best fit between theory and experiment. The measured values of relative capacitance change are in the range of 1–1.34%.

4.2. Stainless steel and titanium diaphragm sensors

Capacitance versus pressure data of the stainless steel and titanium diaphragm sensors are shown in Fig. 8. For a range of applied pressure from 0 to 178 kPa, the net capacitance change for stainless steel was 0.14 pF and for titanium it was 0.25 pF. The sensitivities of the stainless steel diaphragm sensors were approximately 9.03 ppm/kPa and for titanium were approximately 27.00 ppm/kPa. The sensitivities are much smaller than for the Kapton diaphragm pressure sensor due to the higher modulus of elasticity of the metal diaphragm. Although, the combined electromechanical model of Eqs. (3), (5) and (9) predicted the behavior of the Kapton diaphragm sensors well, it did not predict the behavior of the metallic diaphragm sensors well. In order to determine whether the electrical or the mechanical behavior was deviating from the theoretical predictions, the center deflection of the diaphragm as a function of pressure was measured directly. These measurements were performed by removing the sensor backplates upon completion of the capacitance measurements, repeating the pressurization, and observing in a microscope the extent of lateral deflection due to the applied pressure. The deflection data for the stainless steel and titanium diaphragms are shown in Fig. 9, where *up1* refers to data from a sample diaphragm under increasing pressure and *down1* refers to data from the same diaphragm under decreasing pressure. *Up2* and *down2* refers to similar data from a second diaphragm. As can be seen from Fig. 9, the mechanical model predictions overestimate the measured diaphragm deflections significantly, even when the effect of stretching of the diaphragm is taken into account as indicated by Eq. (2). It is unlikely that the discrepancy is attributable to simple mechanical yielding as identical deflection results were obtained during a pressurization and depressurization cycle. The other assumptions in the model were zero residual stress and isotropic material properties. Finite element calculations predict the presence of significant amounts of residual stress in the film due to cooling from the lamination temperature. In addition, the metallic diaphragms may have anisotropic characteristics

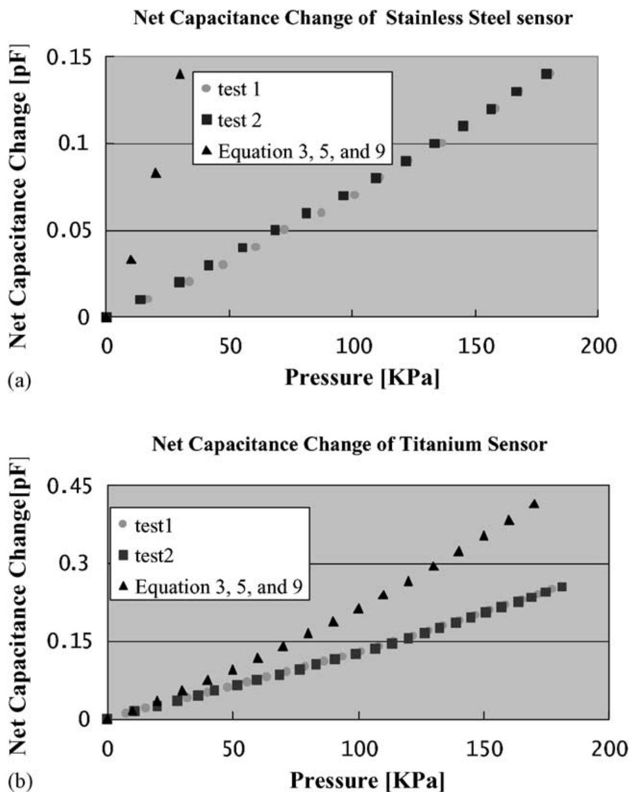

Fig. 8. Net capacitance change versus pressure for metal diaphragm pressure sensor: (a) stainless steel diaphragm pressure sensor; (b) titanium diaphragm pressure sensor.

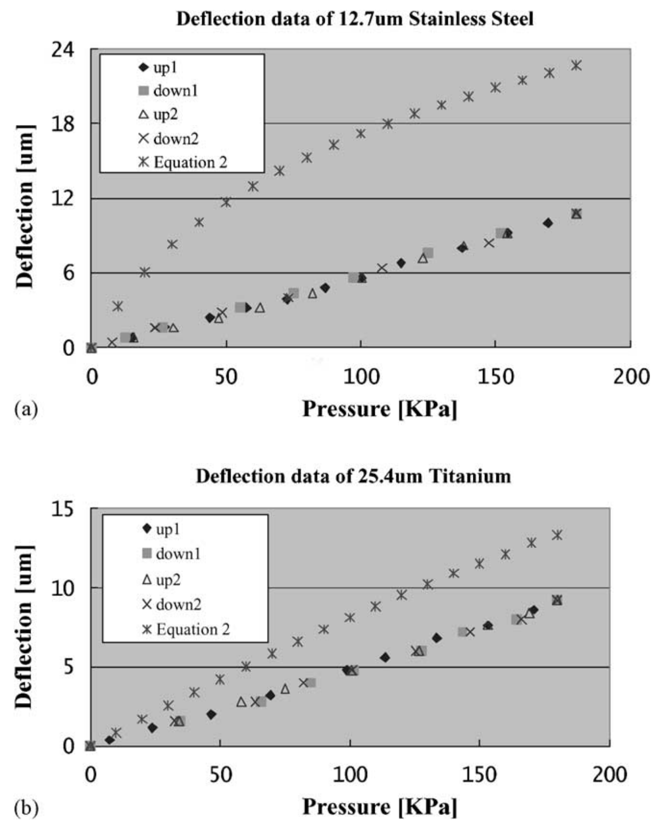

Fig. 9. Metal diaphragm deflection vs. pressure: (a) stainless steel diaphragm; (b) titanium diaphragm.

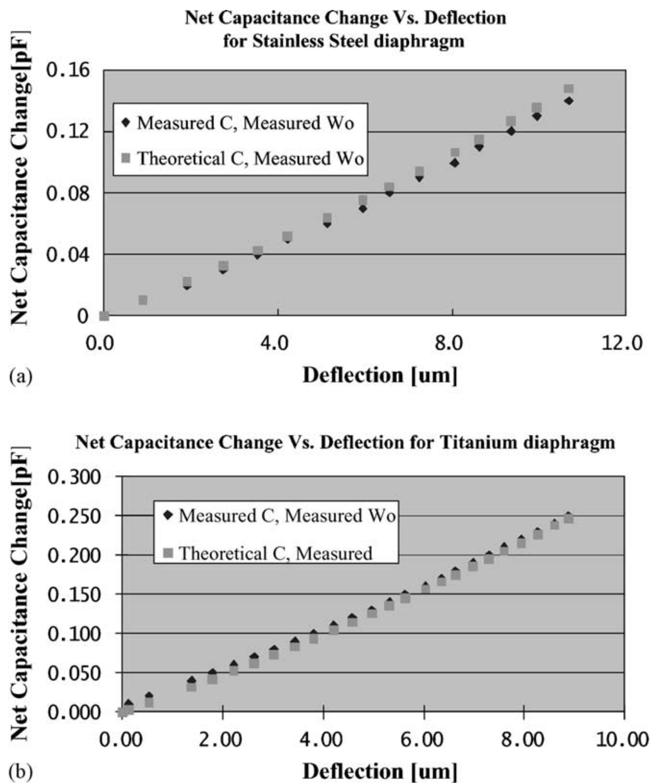

Fig. 10. Net capacitance change vs. deflection: (a) stainless steel diaphragm pressure sensor; (b) titanium diaphragm pressure sensor.

due to the rolling and drawing processes used in their manufacture, as well as strains induced during the lamination process.

To verify that the electrical portion of the modeling was correct the measured deflections shown in Fig. 9 were combined with Eqs. (5) and (9) to yield a prediction of the capacitance of the sensor as a function of pressure. Fig. 10 indicates the capacitance versus deflection for the stainless steel and titanium diaphragms. The deflection was measured for all cases and the capacitance indicates measured and theoretical values. As can be seen, the two sets of plots correspond well with each other. This indicates that given the correct deflection data, the calculated capacitance will match up with the measured capacitance. The summarized data of the three types of capacitive pressure sensors are shown in Table 1.

Table 1
Measured data for three types of capacitive pressure sensors

	Kapton	Stainless steel	Titanium
Diaphragm radius (mm)	1	1	1
Diaphragm thickness (μm)	50	12.7	25.4
Gap (μm)	≈40	≈27	≈21
Back plate dimension (mm)	2.8 × 2.2	3.5 × 3.0	3.5 × 3.0
Applied pressure (kPa)	0–34	0–178	0–178
ΔC (pF)	0.14	0.14	0.25
Sensitivity, $\Delta C/C/P$ (ppm/kPa)	294.75	9.03	27.00

5. Conclusions

Stainless steel has been studied as a robust substrate material for micromachined devices. Lamination combined with traditional micromachining processes has been investigated as suitable fabrication methods for this robust substrate. Three types of capacitive pressure sensors have been designed, fabricated, and characterized by using lamination processing with Kapton polyimide, stainless steel, and titanium films as diaphragms on the stainless steel shim stock substrate. The first one based on Kapton diaphragm gave a net capacitance change of about 0.14 pF over an applied pressure range of 0 to 34 kPa with a maximum sensitivity of 294.75 ppm/kPa. The second type utilizing a stainless steel diaphragm has a sensitivity of 9.03 ppm/kPa with a net capacitance change of 0.14 pF over a range of 0 to 178 kPa. The third device using a titanium diaphragm has a sensitivity of 27.00 ppm/kPa and a net capacitance of 0.25 pF over the same range.

Acknowledgements

The authors would like to acknowledge Martin von Arx and Guang Yuan for their assistance in the modeling and simulation of the device. The support of the staff of the Microelectronics Research Center and GTRI Machine Shop at Georgia Tech is acknowledged. This work was supported by Defense Advanced Research Project Agency (DARPA) and the Air Force Office of Scientific Research (AFOSR) under Contract F49620-97-1-0519.

References

[1] H. Baltes, CMOS micro electromechanical systems, Sens. Mater. 9 (6) (1997) 331–346.
[2] N.C. MacDonald, SCREAM microelectromechanical systems, Microelectr. Eng. 32 (1-4) (1996) 49–73.
[3] R. T. Howe, Applications of silicon micromachining to resonator fabrication, in: Proceedings of the 1994 IEEE International Frequency Control Symposium, The 48th Annual Symposium (Cat. No. 94CH3446-2), 1994, pp. 2–7.
[4] C.H. Mastrangelo, X. Zhang, W.C. Tang, Surface micromachined capacitive differential pressure sensor with lithographically-defined silicon diaphragm, in: Proceedings of the International Solid-State Sensors and Actuators Conference-Transducers'95, Vol. 1, 25–29 June 1995, pp. 612–615.
[5] R.R. Tummala, Fundamentals of Microsystems Packaging, McGraw-Hill, New York, 2001.
[6] Stein et al., Thick film heaters made from dielectric tape bonded stainless steel substrates, in: Proceedings of the ISHM'95, Boston, MA, 1994, pp. 125–129.
[7] S.P. Chang, J.B. Lee, M.G. Allen, An 8 × 8 robust capacitive pressure sensor array, in: Proceedings of the International Mechanical Engineering Congress and Exposition, the Winter Annual Meeting of ASME, 15–20 November 1998, Anaheim, CA.
[8] S. Timoshenko, Theory of Plates and Shells, McGraw-Hill, New York, 1940.
[9] W.H. Ko, et al., A high-sensitivity integrated-circuit capacitive pressure transducer, IEEE Trans. Electron Devices ED-29 (1) (1982) 48–56.

[10] Mario Di Giovanni, Flat and Corrugated Diaphragm Design Handbook, Marcel Dekker, New York, 1982.

Biographies

Sung-Pil Chang received the BS degree in electronic engineering from Sung Kyun Kwan University, Korea in 1991. He received the MS degree in electrical engineering from Georgia Institute of Technology in 1998. Currently, he is working on a PhD project in the MSMA group at Georgia Institute of Technology.

Jeong-Bong Lee received the BS degree in electronics engineering from Hanyang University, Seoul, Korea in 1986, the MS degree and the PhD degree in electrical engineering from Georgia Tech, Atlanta, GA in 1993 and 1997, respectively. Since 1997, he has been a postdoctoral research associate and a research engineer II at Georgia Tech. In January 1999, he became an assistant professor of the Department of Electrical and Computer Engineering at LSU, and in 2001 moved to the University of Texas, Dallas, where he currently holds the rank of assistant professor. His research and teaching have focused on microelectromechanical systems (MEMS).

Mark G. Allen received three bachelor degrees from the University of Pennsylvania in 1983: the BA in chemistry, the BSE in chemical engineering and the BSE in electrical engineering. Following this, he received the SM and PhD degrees in microelectronic materials from the Massachusetts Institute of Technology in l986 and 1989, respectively. He joined the faculty of Georgia Institute of Technology after a postdoctoral appointment at MIT. His main research focus is in microelectromechanical systems (MEMS).